

Applications of the wavelet transform in the generation and analysis of spectrum-compatible records

Luis E. Suárez[†]

*Department of Civil Engineering and Surveying, University of Puerto Rico, Mayagüez,
Puerto Rico 00681-9041, U.S.A.*

Luis A. Montejó[‡]

*Department of Civil Construction and Environmental Engineering, North Carolina State University,
Raleigh, North Carolina 27695-7908, U.S.A.*

(Received August 24, 2005, Accepted June 12, 2007)

Abstract. A wavelet-based procedure to generate artificial accelerograms compatible with a prescribed seismic design spectrum is described. A procedure to perform a baseline correction of the compatible accelerograms is also described. To examine how the frequency content of the modified records evolves with time, they are analyzed in the time and frequency using the wavelet transform. The changes in the strong motion duration and input energy spectrum are also investigated. An alternative way to match the design spectrum, termed the “two-band matching procedure”, is proposed with the objective of preserving the non-stationary characteristics of the original record in the modified accelerogram.

Keywords: spectrum compatible accelerograms; wavelet transform; baseline correction; input energy spectrum; strong motion duration.

1. Introduction

Seismic design forces are usually specified in the form of smooth design response spectra that (hopefully) take into account every possible earthquake likely to occur in a given zone with a certain probability of occurrence. For a single degree of freedom (DOF) oscillator with period T_n and damping ratio ξ , the acceleration ordinate $Sa(T_n, \xi)$ obtained from a response spectrum multiplied by the oscillator's weight gives the maximum shear force at its base or support. By using modal decomposition this approach can be extended to multi DOF systems. There are, however, several instances where acceleration time histories are required as seismic input instead. For example, to determine the ultimate resistance and to identify modes of failure of structures, a nonlinear time history analysis is needed. In other cases, acceleration time histories are required for linear analyses. For instance, many seismic codes require this type of analysis for buildings with pronounced irregularities. Time-history analyses are also required for very tall buildings or for

[†] Professor, Corresponding author, E-mail: lsuarez@uprm.edu

[‡] Research Assistant, E-mail: lamontej@ncsu.edu

critical or “one-of-a-kind” structures. A few codes even make time history analyses compulsory (such as those from Iran, New Zealand, etc.). Moreover, acceleration records are also commonly employed in geotechnical earthquake engineering for ground response analysis.

In these cases, it is common to use acceleration time histories whose response spectra are compatible with the code-prescribed design spectrum. The artificial accelerograms can be generated from the superposition of sine waves with random phases; the resulting amplitude is modulated by a smooth function to account for the transient character of the seismic motions. This is the case of the well known method of Vanmarcke and Gasparini (1976) coded in the program SIMQKE. These methods are perhaps the most attractive for design code applications since the required input, a response spectrum, is almost always available and therefore the criteria for the generation of records are very easily specified.

It has been also proposed to modify recorded (or “seed”) accelerograms so that the response spectra of the revised records match a specified design spectrum. There is a long list of these procedures, which can be broadly classified as time domain or frequency domain methods. Lately, the use of wavelets was also proposed for the same purpose (See for instance: Rizzo *et al.* 1975, Lilhanand and Tseng 1988, Mukherjee and Gupta 2002, Suarez and Montejó 2003, 2005, Hancock *et al.* 2006). All the available methods require a careful selection of the seed accelerograms in order to minimize the adjustments required and to try to retain as much as possible the frequency content of the original records.

The use of the artificial records has been the object of criticism (Naeim and Lew 1995, Bommer and Ruggeri 2002). Since a smooth design response spectrum is not intended to represent the response to a single ground motion event, the characteristics of an artificial record whose response spectrum match a smooth design response spectrum are not realistic. For example, it has been shown that these records tend to have high energy content in a wide range of frequencies.

Since real accelerograms do account for many characteristics of the source, path, and site that influence the nature of strong ground motions, some authors advocated procedures for site-specific analysis based on the selection and scaling of real accelerograms (Bommer and Scott 2000, Malhotra 2003). However, except for those regions of the world where recorded accelerograms are available, in the current engineering practice artificial earthquake records are still preferred for dynamic analysis despite their shortcomings.

A compromise between the use of artificial and real records are synthetic accelerograms which are derived from sophisticated models of seismic fault rupture. Although this type of techniques has several advantages, they are not favored by many practicing engineers, probably due to their complexity.

This paper describes how the continuous wavelet transform can be used to modify historic records so that their spectra match a target response spectrum. The focus is on the practical aspects required for the implementation: a detailed mathematical description of the process and the wavelet used can be found in Suarez and Montejó (2005). The wavelet transform is also used in the present work to investigate the changes introduced in the original signals by the procedure. Moreover, since the method yields accelerograms with non-zero end velocity and displacement, a baseline correction method is explained and applied. Finally, an alternative way to match a target spectrum that can at least partially overcome the disadvantages of the proposed and similar methods is investigated. The procedure, which is referred to as two-band matching procedure, is exemplified with a numerical example.

2. The wavelet transform

The wavelet transform is a two-dimensional linear transform that maps a function of time or space into a “scale” and “position” domain. If the original function depends on time t , then the position, denoted as p , is also a time variable. The scale, identified as s , is approximately proportional to the inverse of the frequency. As with the Fourier transform, there is a continuous and a discrete version of the wavelet transform. For the applications presented in this paper only the continuous transform will be used. The continuous wavelet transform of a signal $f(t)$ is defined by the integral

$$C(s, p) = \int_{-\infty}^{\infty} f(t) \psi_{s,p}(t) dt \quad (1)$$

The function $C(s, p)$ contains information about the function $f(t)$ at the scale s around the time position p . The functions $\psi_{s,p}(t)$ are referred to as the “analyzing wavelets”. They are defined by translating along the time axis and stretching or compressing a so-called “mother wavelet” $\Psi(t)$

$$\psi_{s,p}(t) = \frac{1}{\sqrt{s}} \Psi\left(\frac{t-p}{s}\right) \quad (2)$$

The wavelet $\Psi(t)$ is a localized wave around $p = 0$ that drops to zero after a few oscillations with a null average value. There are only a few mother wavelets that have closed form expressions; most of them are defined by recursive equations. The selection of the proper mother wavelet is crucial for the successful implementation of a given application. For the applications presented in this work, we use the “impulse response wavelet” due to its similarity with the impulse response function of viscously damped oscillator. The mathematical properties and advantages of this wavelet in the analysis of earthquakes records are discussed in Suarez and Montejo (2005) and Hancock *et al.* (2006). The mother wavelet is defined as (Suarez and Montejo 2005)

$$\Psi(t) = e^{-\xi\Omega|t|} \sin\Omega t \quad (3)$$

where ξ and Ω are the parameters that define the shape of the wavelet. For the applications

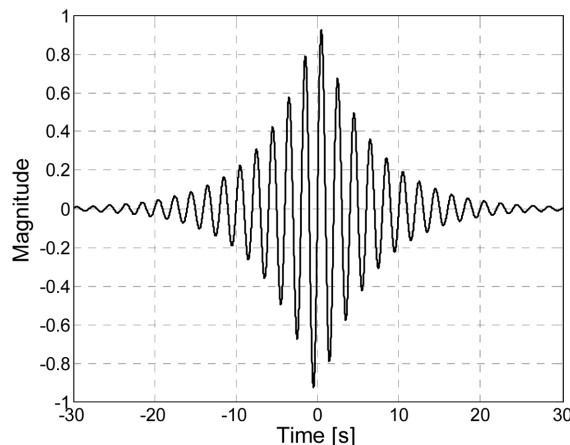


Fig. 1 The impulse response wavelet

presented here, we used $\xi = 0.05$ and $\Omega = \pi$. Fig. 1 shows the proposed impulse response wavelet for these two values of the parameters ξ and Ω . Although this wavelet is similar to the real version of the Morlet wavelet (Misiti *et al.* 2000), for the applications we are interested in, the wavelet in Eq. (1) yielded the best results. This confirms a well known fact in wavelet analysis, namely that there is no ubiquitous wavelet appropriate for all applications but rather the proper wavelet must be sought for each case.

In many applications one is interested in recovering the original function $f(t)$, usually after processing it to achieve some objective. This can be done with the inverse wavelet transform which is defined by the “reconstruction formula”

$$f(t) = \frac{1}{K_\psi} \int_{s=0}^{\infty} \left(\int_{p=-\infty}^{\infty} C(s, p) \psi_{s,p}(t) \frac{dp}{s^2} \right) ds \quad (4)$$

where K_ψ is a constant that depends on the mother wavelet.

The functions within parenthesis in Eq. (4) will be referred to as the “detail functions” $D(s, t)$. In terms of them, the function can be written as

$$f(t) = \frac{1}{K_\psi} \int_0^{\infty} D(s, t) ds \quad (5)$$

Although the detail functions are not harmonic, they have a dominant frequency that depends on the type of wavelet. For the proposed impulse response wavelet, the dominant frequency and period for each detail function can be defined as follows. The analyzing wavelet is

$$\psi_{s,p}(t) = \psi\left(\frac{t-p_n}{s_j}\right) = e^{-\xi\Omega\left|\frac{t-p_n}{s_j}\right|} \sin\left(\frac{\Omega t - p_n}{s_j}\right) \quad (6)$$

and examining this function we can write

$$\omega_j = \frac{\Omega}{s_j}, \quad T_j = \frac{2\pi}{\Omega} s_j; \quad j = 1, 2, \dots, N \quad (7)$$

3. Generation of the artificial earthquakes

The proposed spectrum-matching procedure is based on the wavelet decomposition of a recorded accelerogram into a finite number of detail functions with a dominant frequency. The detail functions are then scaled up or down iteratively such that the reconstituted function is compatible with a specified design spectrum. The step-by-step operations required to implement the procedure are described next:

1. Read the earthquake data file $\ddot{X}_g(t_k)$ sampled at Nt points and prescribe the smooth response spectrum that the modified accelerogram is required to match. The spectrum is defined for a fixed damping ratio. Even though the procedure could be applied to any accelerogram, it is advisable to choose one that has a duration compatible with the controlling seismic events.
2. Define the discrete parameters s (scale) and p (position) as follows

$$s_j = \frac{\Omega}{2\pi} T_j \quad (8)$$

$$p_n = n \cdot \Delta p; \quad n = 0, 1, \dots, Nt = \frac{t_f}{\Delta t} \quad (9)$$

The times t_f and Δt are the final time and the sampling rate of the accelerogram, respectively, $\Delta p = \Delta t$ and $\Omega = \pi$, as specified earlier. The values for the periods T_j should be defined based on the spectral ordinates where the user wants a good match between the target and response spectra.

3. Calculate the continuous wavelet transform using the following discrete approximation of Eq. (1)

$$C(s_j, p_n) \cong \frac{\Delta t}{\sqrt{s_j}} \sum_{k=1}^{Nt} \ddot{X}_g(t_k) \psi\left(\frac{t_k - p_n}{s_j}\right) \quad (10)$$

4. Calculate the “detail functions” $D(s, t)$ as follows

$$D_j(t) = \frac{\Delta t}{s_j^{5/2}} \sum_{n=1}^{Nt} C(s_j, p_n) \psi\left(\frac{t - p_n}{s_j}\right) \quad (11)$$

5. Reconstruct the accelerogram by adding the details functions as in Eq. (5) with the scaling constant $K_\psi = 1$

$$\ddot{X}_g(t) \cong \sum_{j=1}^{N-1} D_j(t) \cdot \Delta s_j \quad (12)$$

6. Calculate the ground response spectrum of the reconstructed signal $\ddot{X}_g(t)$ at the values of the periods T_j defined by the discrete values of s_j in Eq. (8). Then compute the ratios γ_j between the values of the target $[Sa(T_j)]_{target}$ and calculated spectra $[Sa(T_j)]_{reconstructed}$

$$\gamma_j = \frac{[Sa(T_j)]_{target}}{[Sa(T_j)]_{reconstructed}} \quad (13)$$

7. Multiply the detail functions $D_j(t)$ by these ratios and obtain a new accelerogram using Eq. (12). Calculate the response spectrum of this updated accelerogram, compute a set of new ratios γ_j and correct the previous detail functions. The process continues until the ratios γ_j become sufficiently close to 1 or a pre-established maximum number of iterations is reached.
8. At every iteration step, verify the convergence of the process using as measure of the error the Root-Mean-Square of the differences between the spectral values at each period

$$e(\%) = \sqrt{\frac{1}{N} \sum_{j=1}^N \left(\frac{S_a(T_j)_{target} - S_a(T_j)_{reconstructed}}{S_a(T_j)_{target}} \right)^2} * 100 \quad (14)$$

To illustrate the proposed procedure, the records of three earthquakes with different characteristics were selected. It is desired to modify these records so they will be compatible with the ground design spectrum prescribed in the Uniform Building Code (UBC), 1997 Edition (ICBO 1997) for a seismic zone 3 and soil type SB (rock). The example motions are those of the: (i) Coalinga earthquake (California 1983) measured at Oil Fields Fire Station; (ii) Loma Prieta earthquake (California 1989) registered at Treasure Island and (iii) Coyote Lake earthquake (California 1979)

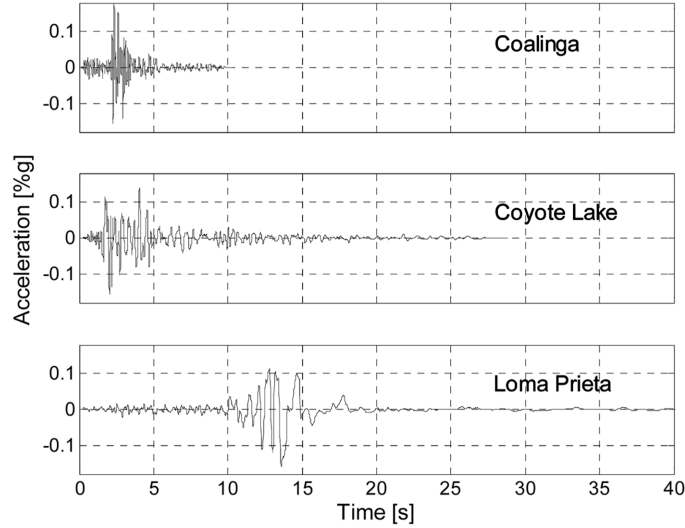


Fig. 2 Original records of the Coalinga, Coyote Lake and Loma Prieta earthquakes

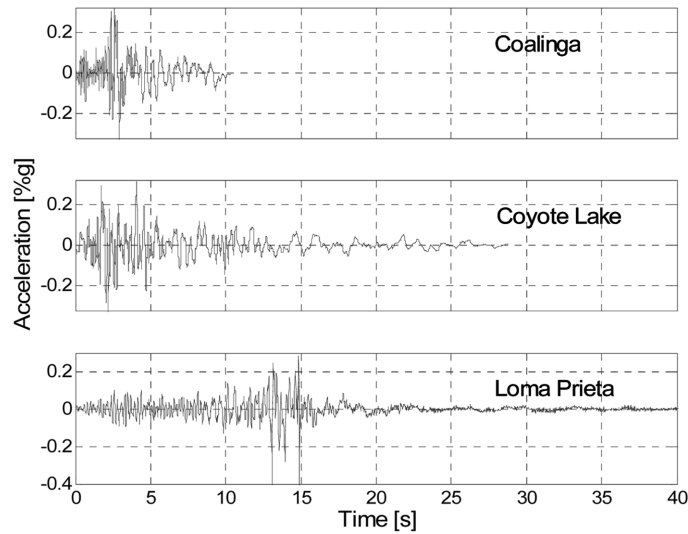


Fig. 3 Modified records of the Coalinga, Coyote Lake and Loma Prieta earthquakes

recorded at Coyote Lake Dam – San Martín. Fig. 2 shows the original accelerograms. The spectrum-compatible accelerograms obtained with the procedure are displayed in Fig. 3.

Figs. 4 to 6 show the selected UBC-97 design spectrum, the response spectrum of the original record, and the final spectrum after applying the proposed procedure for each of the three earthquake records. Usually an acceptable convergence (RMS error less than 5%) is obtained with less than ten iterations. The spectral values in Figs. 4 to 6 were evaluated at equally spaced periods with 0.05s interval. These are not necessarily equal to the periods T_i used in the procedure to decompose the signals with the wavelet transform. It is relevant to mention here that it is not necessary to match the smooth target spectrum as exactly as possible. The match should be

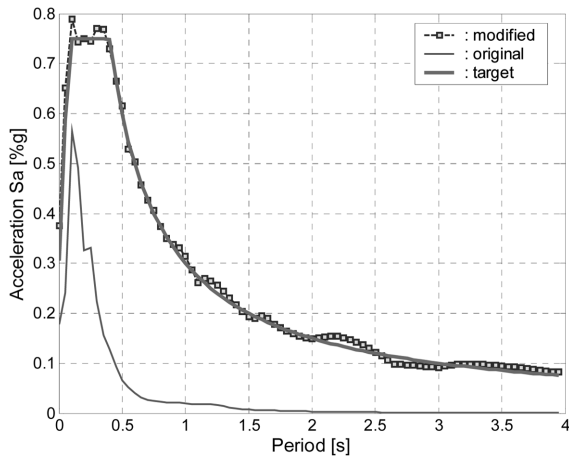


Fig. 4 The target spectrum and the spectra of the original and modified record of the Coalinga earthquake

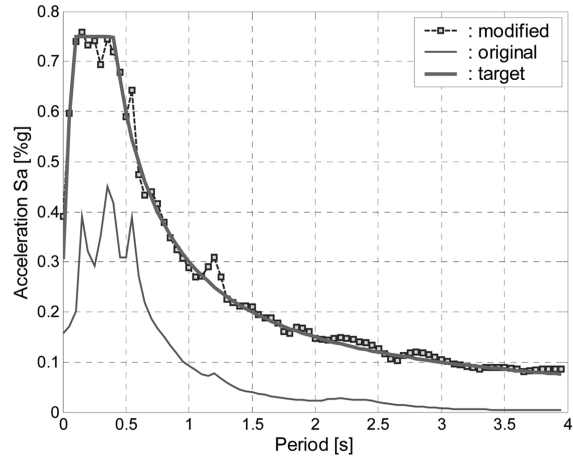


Fig. 5 The target spectrum and the spectra of the original and modified record of the Coyote Lake earthquake

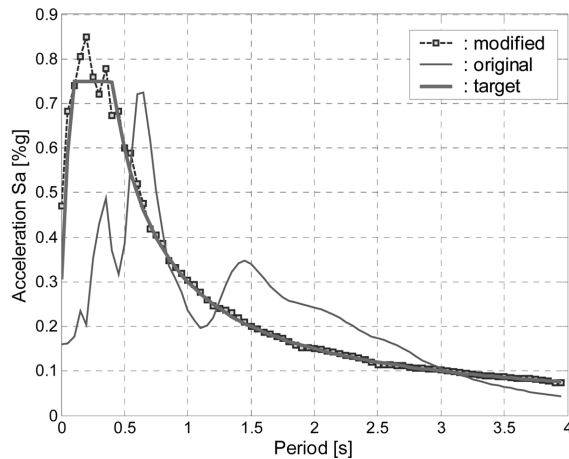


Fig. 6 The target spectrum and the spectra of the original and modified record of the Loma Prieta earthquake

achieved only in an average sense, since the spectra of all real ground motion are never smooth. Moreover, when matching a code design spectrum such as the 1997 UBC, one must have in mind that these spectra usually do not correspond to a single earthquake. In fact, the short, medium and long period spectral accelerations are generally obtained as the average or envelope of different set of earthquakes. Therefore, it may not be reasonable to match the entire spectrum with a single acceleration time history. To address this issue a “two band matching procedure” is presented in a later section.

4. Baseline correction

Fig. 7 shows the displacement and velocity time-histories obtained via trapezoidal integration of

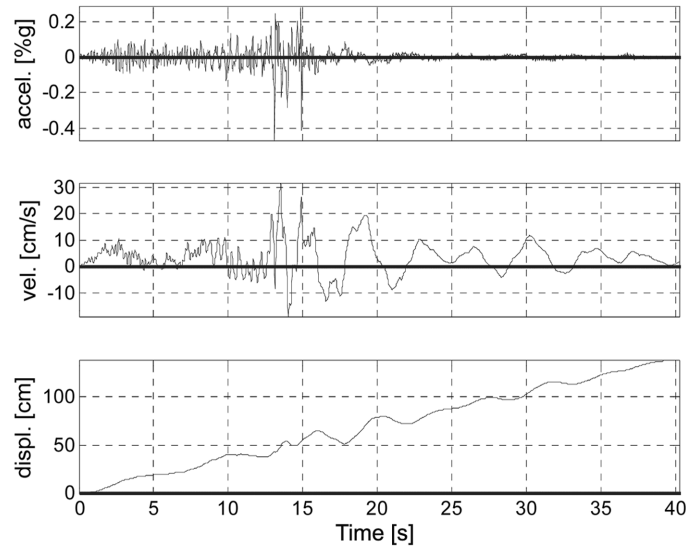


Fig. 7 Velocity and displacement obtained by numerical integration of the modified acceleration record of the Loma Prieta earthquake

the UBC-97 spectrum compatible accelerogram of the record of the Loma Prieta earthquake. It is evident that the results obtained are unrealistic and physically impossible: for example, the ground displacement trace shown in Fig. 7 never crosses the zero line and it has a permanent displacement of 140 cm at the end. Therefore, the wavelet based procedure must be complemented by a baseline correction scheme. The loss of baseline correction is a common feature of many methods for generation of artificial earthquakes, such as the SIMQKE, and thus caution must be exercised when applying these procedures.

Seismograph records are usually corrected by a step-by-step time-domain process, such as the methods developed at the Caltech (Trifunac and Lee 1976) and further adapted by the U.S Geological Survey (Converse *et al.* 1984). In principle, any of the methods available in the literature can be used for the correction of spectrum-compatible records. However, care should be exercised when applying a given scheme, since some baseline correction methods modify the frequency content of the record, and thus their use to amend a spectrum compatible accelerogram could result in a non-compatible record after the correction. A method to apply a baseline correction that is able to maintain the compatibility of acceleration records with the target spectrum is described and applied here.

The following procedure to correct the raw accelerogram was briefly cited in an appendix of a book by Wilson (2001). There are no detailed explanations of the procedure in this reference and therefore, a complete explanation of the procedure and its basis are provided next.

The procedure presented next can be applied to obtain a record with both zero end velocity and zero end displacement. However, it is realized that in some cases there could be a permanent ground deformation after the earthquake. In this case, the final ground displacement can be constrained to take a preselected non-zero value u_{perm} .

A typical earthquake acceleration time series can be approximately considered as a sum of acceleration pulses, such as the one shown in Fig. 8. The velocity produced by a single acceleration

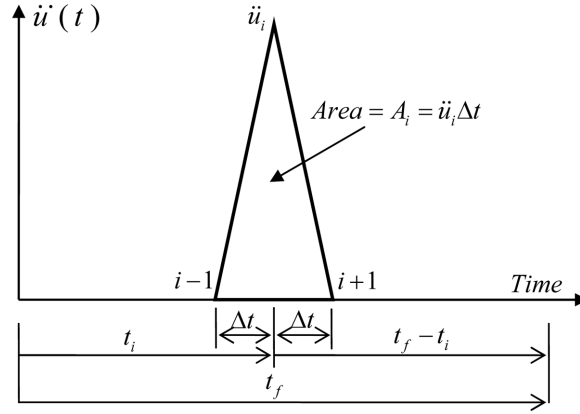


Fig. 8 A typical earthquake acceleration pulse

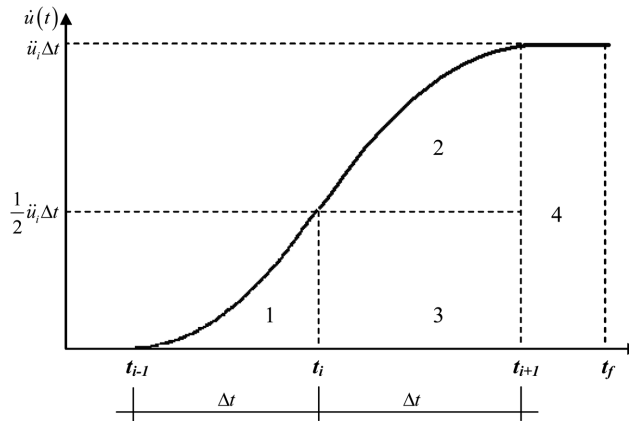


Fig. 9 Velocity as a function of time for a triangular acceleration pulse

pulse is given by the area A_i of the pulse. If the acceleration pulse is triangular as shown in Fig. 8, the area is $A_i = \ddot{u}_i \Delta t$. Therefore, for the complete record, one can calculate the exact end velocity as the sum of the areas of the pulses A_i over the accelerogram

$$\dot{u}_f = \sum_{i=1}^f \ddot{u}_i \Delta t = \Delta \dot{U} \quad (15)$$

where $\Delta \dot{U}$ is the non-zero value that needs to be corrected.

Fig. 9 shows the velocity as a function of time due to the single acceleration pulse displayed in Fig. 8. During the first interval Δt , the velocity is given by a parabolic spandrel obtained by integrating the linear acceleration from t_{i-1} to t

$$\dot{u}(t) = \frac{1}{2} \frac{\ddot{u}_i}{\Delta t} (t - t_{i-1})^2 \quad (16)$$

The velocity at a time $t_i \leq t \leq t_{i+1}$ is given by the parabolic equation

$$\dot{u}(t) = -\frac{1}{2}\frac{\ddot{u}_i}{\Delta t}(t-t_{i-1})^2 + \ddot{u}_i(t-t_i) + \frac{1}{2}\ddot{u}_i\Delta t \quad (17)$$

The displacement at the end of the interval t_f due to the single acceleration pulse in Fig. 8 is the area under the curve in Fig. 9. This can be calculated as the sum of the four areas identified as 1, 2, 3 and 4 in this figure

$$\begin{aligned} A_1 &= \frac{1}{6}\ddot{u}_i\Delta t^2; & A_2 &= \frac{1}{3}\ddot{u}_i\Delta t^2 \\ A_3 &= \frac{1}{2}\ddot{u}_i\Delta t^2; & A_4 &= \ddot{u}_i\Delta t[t_f - (t_i + \Delta t)] \end{aligned} \quad (18)$$

The displacement at the end of the record (i.e., at time t_f) due to the single pulse at time t_i is the sum of the four areas, i.e.

$$(u_f)_i = \sum_{k=1}^4 A_k = \ddot{u}_i\Delta t(t_f - t_i) \quad (19)$$

The displacement at time t_f due to the different pulses that form the accelerogram is the sum of the displacements in Eq. (19).

$$u_f = \sum_{i=1}^f (u_f)_i = \sum_{i=1}^f (t_f - t_i)\ddot{u}_i\Delta t = \Delta U \quad (20)$$

The quantity ΔU in Eq. (20) is the non-zero displacement that we are seeking to correct. If it is desired to obtain a final ground displacement u_{perm} , then the right-hand-side of Eq. (20) should be set equal to $\Delta U - u_{perm}$. In this case, ΔU is the error in the artificial record and u_{perm} is the actual permanent ground displacement.

The main idea of the method is to correct a small subset of the discrete acceleration values \ddot{u}_i such that the final velocity and, if desired, the final displacement are zero. It is proposed first to correct the first t_L seconds of the accelerogram to achieve zero displacement at the end of the record. Since the time t_L is $L\Delta t$, this implies that the first “ L ” data points of the record will be corrected. From Eq. (20), the corrected displacement u_f^c at the end of the record can be calculated as follows

$$u_f^c = \sum_{i=1}^L (t_f - t_i)g_i\ddot{u}_i\Delta t + \sum_{i=1}^L (t_f - t_i)\ddot{u}_i\Delta t + \sum_{i=L+1}^f (t_f - t_i)\ddot{u}_i\Delta t \quad (21)$$

where g_i are the weights used to correct the first L values of the accelerogram. We know that the second and third summation terms give ΔU (or $\Delta U - u_{perm}$), and thus to obtain $u_f^c = 0$ (or $u_f^c = u_{perm}$) we require

$$\sum_{i=1}^L (t_f - t_i)g_i\ddot{u}_i\Delta t = -\Delta U \quad (22)$$

The simplest way to correct the acceleration points, i.e., to define the weights g_i , is to use a linear function $g(t)$. To avoid a discontinuity in the acceleration record, the linear function should decrease from a certain value at time $t = 0$ to zero at time $t = t_L$. Thus the linear function is defined as

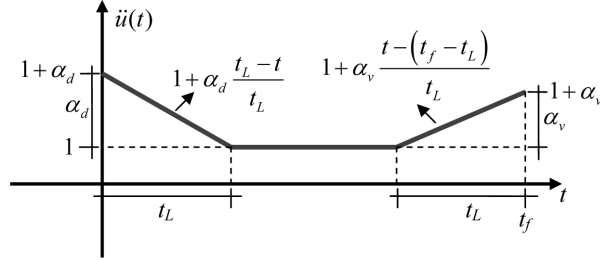


Fig. 10 Correction functions to set displacement and velocity zero at the end of the accelerogram

$$g(t) = \alpha_d \frac{t_L - t}{t_L}; \quad 0 \leq t \leq t_L \quad (23)$$

The function $g(t)$ is shown in Fig. 10. Since the times are sampled at constant intervals Δt , substituting t_L and t by the discrete times $L\Delta t$ and $\Delta t(i-1)$ we obtain the weights g_i in Eq. (22)

$$g_i = \alpha_d \frac{L - (i-1)}{L}; \quad 1 \leq i \leq L \quad (24)$$

The factor α_d can be obtained by substituting Eq. (24) in Eq. (22), which leads to

$$\alpha_d \sum_{i=1}^L \frac{L - (i-1)}{L} (t_f - t_i) \ddot{u}_i \Delta t = -\Delta U \quad (25)$$

Once this factor is obtained, the correction weights are applied to the first L points of the original accelerogram. Recalling Eqs. (21) and (24), the corrected values of the acceleration are

$$\ddot{u}_i^c = (1 + g_i) \ddot{u}_i = \left(1 + \alpha_d \frac{L-i}{L}\right) \ddot{u}_i; \quad i = 1, \dots, L \quad (26)$$

This, in principle, should be sufficient to obtain a zero (or u_{perm}) displacement at the end of the record. However, it is proposed to define two different factors α_{dp} and α_{dn} for the positive and negative values of the acceleration \ddot{u}_i . This is done to minimize the changes to the accelerogram: using a single factor will alter more the original values \ddot{u}_i . Since there are no additional equations to determine the two factors, it is proposed to define them as follows. Considering only the positive values of \ddot{u}_i in the summation in Eq. (25), the coefficient α_{dp} can be obtained from

$$\alpha_{dp} = \frac{-\Delta U}{2\Delta t} \left[\sum_{i=1}^L \frac{L - (i-1)}{L} (t_f - t_i) (\ddot{u}_i)_+ \right]^{-1} \quad (27)$$

where $(\ddot{u}_i)_+$ are the positive values of the sequence \ddot{u}_i .

The coefficient α_{dn} can be obtained using a similar expression but including only the negative values of \ddot{u}_i , identified as $(\ddot{u}_i)_-$

$$\alpha_{dn} = \frac{-\Delta U}{2\Delta t} \left[\sum_{i=1}^L \frac{L - (i-1)}{L} (t_f - t_i) (\ddot{u}_i)_- \right]^{-1} \quad (28)$$

The corrected acceleration values \ddot{u}_i^c are still given by the Eq. (26) but now if the original \ddot{u}_i is

positive, α_d must be replaced by α_{dn} , and vice versa, if it is negative α_{dp} must be used.

The next task is to correct the acceleration such that the velocity at the end of the record is zero. It is proposed to modify now the last “ L ” values of \ddot{u}_i (i.e., the last t_L seconds of the accelerogram). From Eq. (15), the corrected velocity at the end of the record can be written as

$$\dot{u}_f^c = \sum_{i=1}^{f-L-1} \ddot{u}_i \Delta t + \sum_{i=f-L}^f \ddot{u}_i \Delta t + \sum_{i=f-L}^f h_i \ddot{u}_i \Delta t \quad (29)$$

where the weights h_i are used to correct the last “ L ” terms \ddot{u}_i . The first two terms in Eq. (29) are equal to $\Delta \dot{U}$, i.e., to the error in the end velocity. This value will be corrected with the last term. Here again a linear function $h(t)$, shown in Fig. 10, will be used to define the weights: the continuous time function and the weights h_i are

$$h(t) = \alpha_v \frac{t - (t_f - t_L)}{t_L}; \quad t_f - t_L \leq t \leq t_f \quad (30)$$

$$h_i = \alpha_v \frac{i - (f - L + 1)}{L}; \quad f - L + 1 \leq i \leq f \quad (31)$$

The coefficient α_v is obtained by requiring that the first summation in Eq. (29) be equal to the last two terms, that is

$$\alpha_v \sum_{i=f-L+1}^f \frac{i - (f - L + 1)}{L - 1} \ddot{u}_i \Delta t = -\Delta \dot{U} \quad (32)$$

The acceleration record corrected for zero end velocity is given by

$$\ddot{u}_i^c = (1 + h_i) \ddot{u}_i = \left(1 + \alpha_v \frac{i - (f - L + 1)}{L} \right) \ddot{u}_i; \quad i = f - L + 1, \dots, f \quad (33)$$

As it was done to obtain zero end displacement, it is proposed to use two coefficients α_v : the first coefficient α_{vp} will correct the positive values of \ddot{u}_i and another one α_{vn} will be applied to correct the negative values.

The coefficient α_{vp} is computed by using only the positive values of \ddot{u}_i , identified as $(\ddot{u}_i)_+$, in the following summation

$$\alpha_{vp} = \frac{-\Delta \dot{U}}{2\Delta t} \left[\sum_{i=f-L+1}^f \frac{i - (f - L + 1)}{L - 1} (\ddot{u}_i)_+ \right]^{-1} \quad (34)$$

Whereas the coefficient α_{vn} is obtained by including only the negative values of \ddot{u}_i , identified as $(\ddot{u}_i)_-$

$$\alpha_{vn} = \frac{-\Delta \dot{U}}{2\Delta t} \left[\sum_{i=f-L+1}^f \frac{i - (f - L + 1)}{L - 1} (\ddot{u}_i)_- \right]^{-1} \quad (35)$$

The coefficient α_{vp} replaces α_v in Eq. (33) if \ddot{u}_i is positive and, on the contrary, if the original acceleration is negative, α_{vn} must be used to calculate \ddot{u}_i^c .

Using two formulas first, say Eqs. (27) and (28), will correct the end displacement but when the second formulas (Eqs. (34) and (35)) are applied, the previously corrected displacement will not

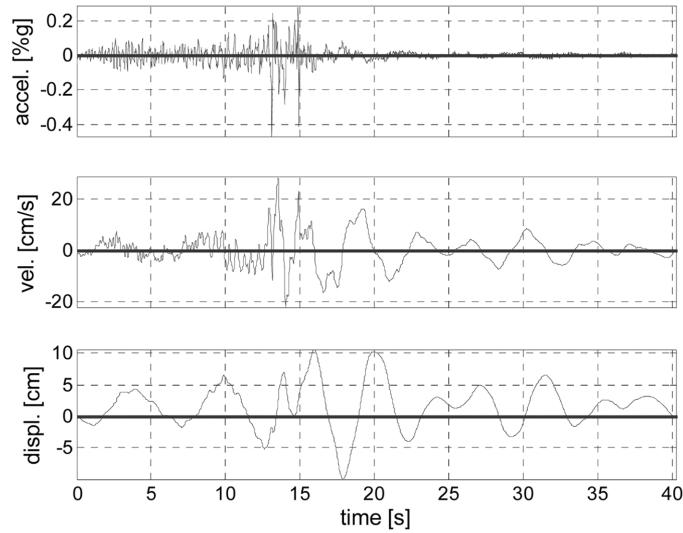


Fig. 11 Velocity and displacement of the modified acceleration record of the Loma Prieta earthquake after the baseline correction

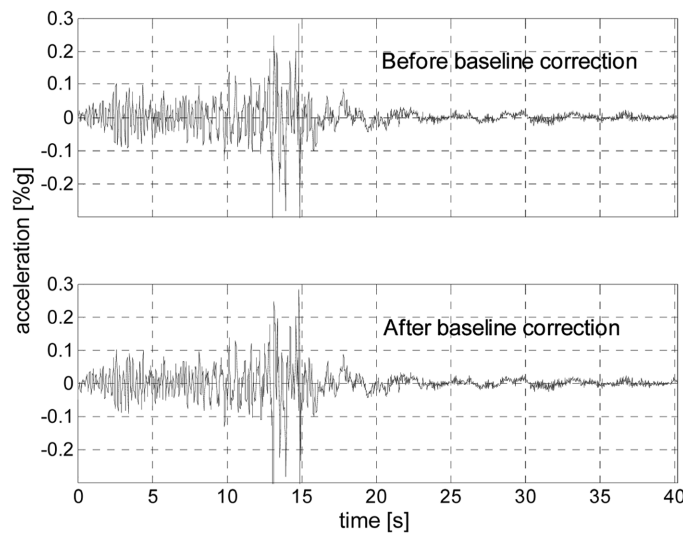


Fig. 12 The records of the Loma Prieta earthquake, before and after the baseline correction

longer be zero. Therefore, an iterative procedure must be implemented to achieve both zero end displacement and velocity, using a pair of formulas at a time.

To illustrate the procedure previously described, the modified record of the Loma Prieta earthquake is corrected. The acceleration, displacement and velocity records obtained are shown in Fig. 11.

The form of the accelerograms remains practically unaltered after the baseline correction since the correction is only applied to a few points at the beginning and end of the record. This can be verified in Fig. 12 which shows the modified accelerograms of Loma Prieta before and after the

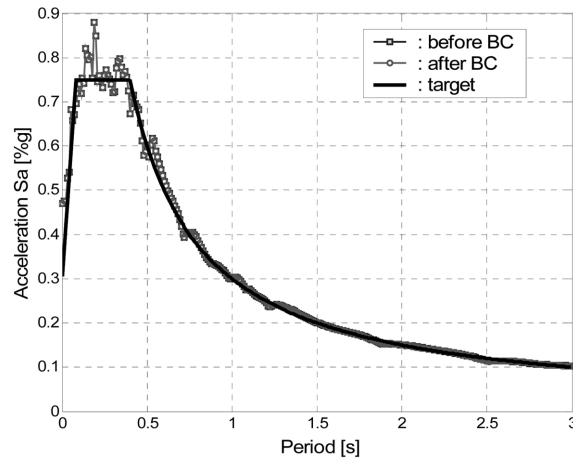


Fig. 13 The target spectrum and the spectra of the modified record of Loma Prieta before and after performing the baseline correction

baseline correction has been performed.

In order to confirm that the corrected records are still compatible with the target spectrum, Fig. 13 displays the response spectra of the Loma Prieta accelerograms before and after the baseline correction was performed. It is evident from this graph that the response spectrum of the artificial record remains compatible after the correction.

6. Analysis of earthquake records in the time-frequency domain

It would be desirable that when a record of a historic ground motion is modified to generate a spectrum compatible accelerogram, the most important temporal variations in the frequency content of the original accelerogram were retained. This, in general, is not possible and some of the attributes that make up the signal will be lost. Thus, at least the temporal variations in each frequency band should be preserved to maintain intact the non-stationary characteristics. It is important then to examine in detail how do the modified records change, in terms of their overall frequency content, non-stationary character, and strong motion duration.

The Fourier transform has been the traditional tool for frequency analysis of ground motion signals. However, for certain applications, the Fourier-based analysis has a weakness. In transforming to the frequency domain, time information is lost: when looking at a Fourier transform of a signal, it is impossible to tell when a particular event took place. If the signal properties do not change much over time (a stationary signal), this drawback is not important. However, if the earthquake record contains non-stationary and transitory characteristics, the Fourier analysis cannot detect them. A combined time-frequency representation of the signal is required to dissect and interpret strongly non-stationary signals. This is done by mapping a one dimensional signal in the time domain into a two dimensional time frequency domain. The wavelet transform is one of the methods that can be used for time-frequency analysis of earthquake records. Here the previously introduced impulse response wavelet is used for this purpose. A “wavelet map” will be used to display how the frequency content of the signals evolves with time. This is a two-dimensional plot

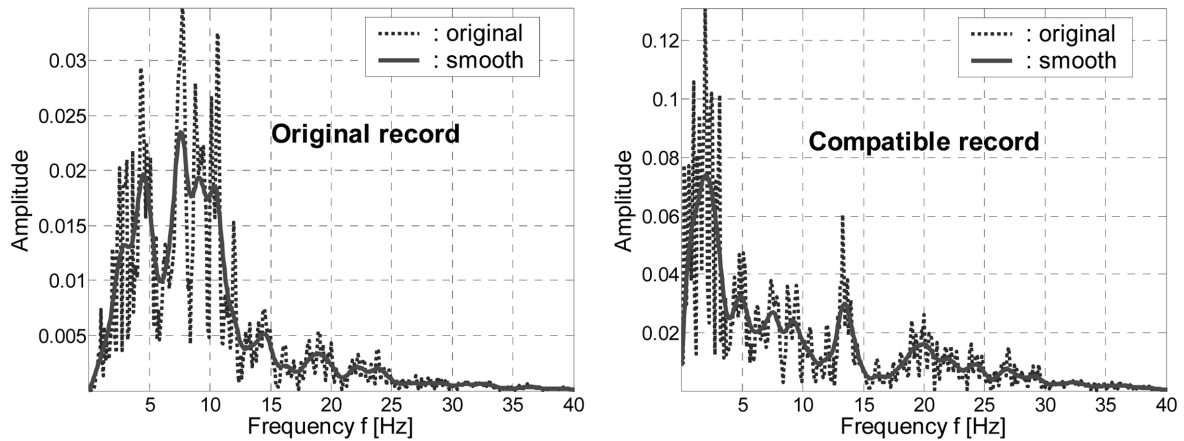


Fig. 14 Fourier Spectrum of the original and modified record of the Coalinga earthquake

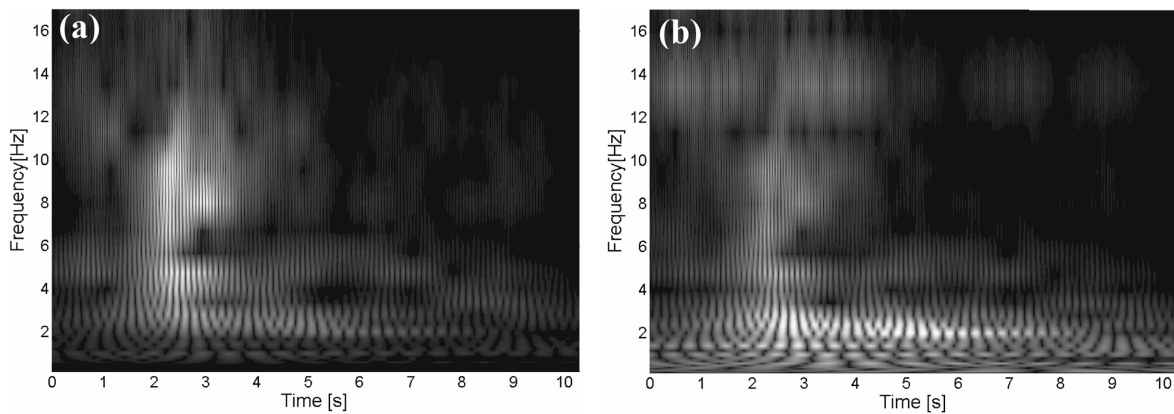


Fig. 15 Wavelet map of the original (a) and modified (b) record of the Coalinga earthquake

of the absolute values of the wavelet coefficients $C(s, p)$ defined in Eq. (1), in which the lighter colors are associated with higher values.

Figs. 14 and 15 show, respectively, the Fourier spectra and the wavelet maps of the original and modified accelerograms of the Coalinga earthquake. These figures reveal that the original record has a dominant frequency around 8 Hz that occurs between the 2nd and the 3rd second. The spectrum of the modified record shows a dominant frequency at about 2 Hz, which starts at about 2.5 seconds and lasts for 4 seconds. Evidently, the frequency content and non-stationary characteristics of the modified accelerograms are different from these of the original accelerograms used as starting point for their generation. Although these changes were observed in all earthquake records used (Montejo 2004), the change in frequency content is more evident in those accelerograms whose original response spectrum is very far from the target spectrum. This occurs because the only parameter that the procedure can modify is the relative importance of the components of different frequencies that make up the accelerogram. It can be argued that when the frequency content and strong motion duration of the original record are modified, the new record no longer represents an earthquake with the same epicentral distance, fault type, etc., than the one initially chosen. This argument is, in

principle, correct but this is a weakness common to all the techniques for generation of spectrum compatible earthquake records. A variant of the proposed procedure that can partially offset this disadvantage is presented later.

A word of caution is in order when examining a wavelet map such as that presented in Fig. 15. Due to the use of the same mother wavelet throughout the analysis, two phenomena referred to as overlapping and distortion can occur. These may hide the identification of the precise time and frequency properties of the inspected signal (Tse *et al.* 2004). In addition, another phenomenon referred to as interference may impede to obtain a good time and frequency resolution specially if there are components of the signal with low energy (Peng *et al.* 2002). These three phenomenon can be minimized with the “exact wavelet analysis” (Tse *et al.* 2004) and the “reassigned wavelet scalogram” (Peng *et al.* 2002). However, the application of these techniques is beyond the scope of the present paper.

7. Strong motion duration of the modified records

It is well known that the strong motion duration of shaking can have a significant effect on the seismic response of structures and soil systems. For instance, it has a strong effect on the inelastic deformation and in the energy dissipation demands of relatively weak, short-period structures (Mahin 1984) and in the occurrence of soil liquefaction. Whether the accelerograms used to deal with these cases are selected from databanks of real earthquake records or generated synthetically, it is important to ensure that the duration of shaking is consistent with the design scenario. The effect of the wavelet-based method on the strong motion duration of the historic records will be briefly examined here.

The Arias intensity, AI (Arias 1970), is used to measure the strong shaking phase of accelerograms. This quantity is a measure of the accumulation of energy in an accelerogram and thus it is defined as the integral of the square of the ground acceleration time history $a(t)$

$$AI = \frac{\pi}{2g_o} \int_0^{t_r} a^2(t) dt \quad (36)$$

where t_r is the total duration of the accelerogram and g is the acceleration due to gravity.

The “significant duration” is then defined as the interval over which some proportion of the total integral is accumulated. This concept has the advantage that it considers the characteristics of the entire accelerogram and defines a continuous time window in which the motion may be considered as strong. In the present work the duration is defined as the interval between the times at which 5% and 95% of the total integral is attained (Trifunac and Brady 1975).

Fig. 16 shows the Husid plots for the original and modified record of the Coalinga earthquake. Examining the two plots it is clear that the strong motion duration was increased after the original record was modified. Similar results were obtained for other time histories.

Observing the Husid plot of the modified record in Fig. 16(b), it can be observed that there are at least three changes in slope between the 5% and the 95% intensities. Figs. 17 and 18 display, respectively, the wavelet map above the Husid plot for the original and spectrum compatible accelerogram. In the original record, the slope of the Husid plot between 5 and 95% is approximately constant. As it can be seen in the wavelet map in Fig. 17, the dominant frequencies are centered around 8 Hz. In the Husid plot of the modified record, there is a steep increase in the

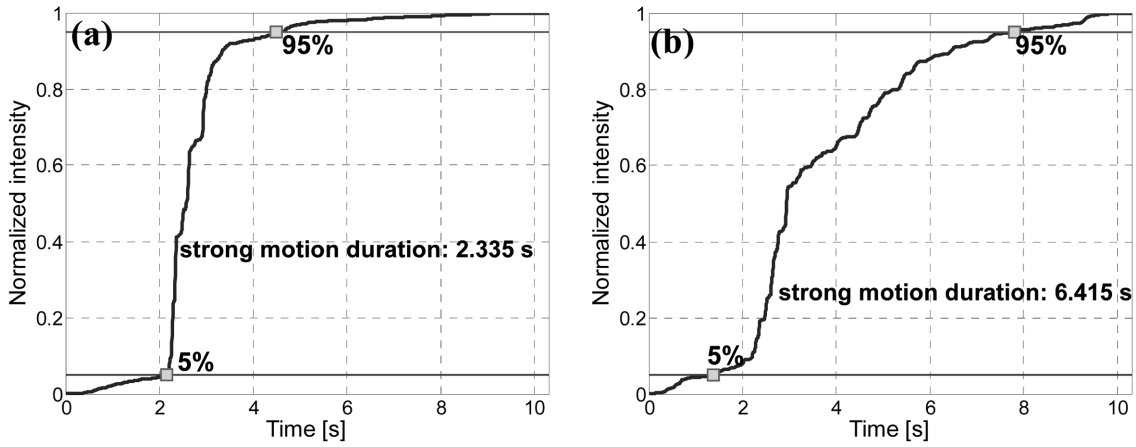


Fig. 16 Husid plots for the original (a) and modified (b) record of the Coalinga earthquake

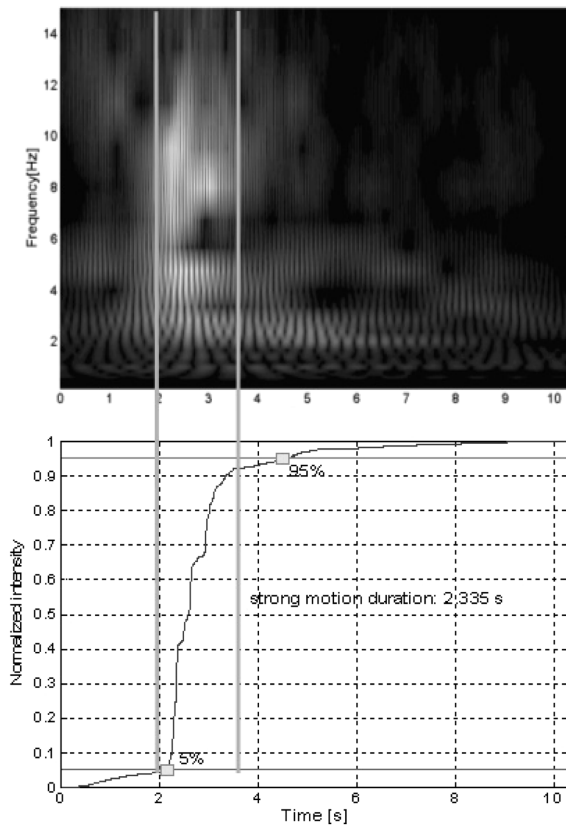


Fig. 17 Wavelet map and Husid Plot of the original record of the Coalinga earthquake

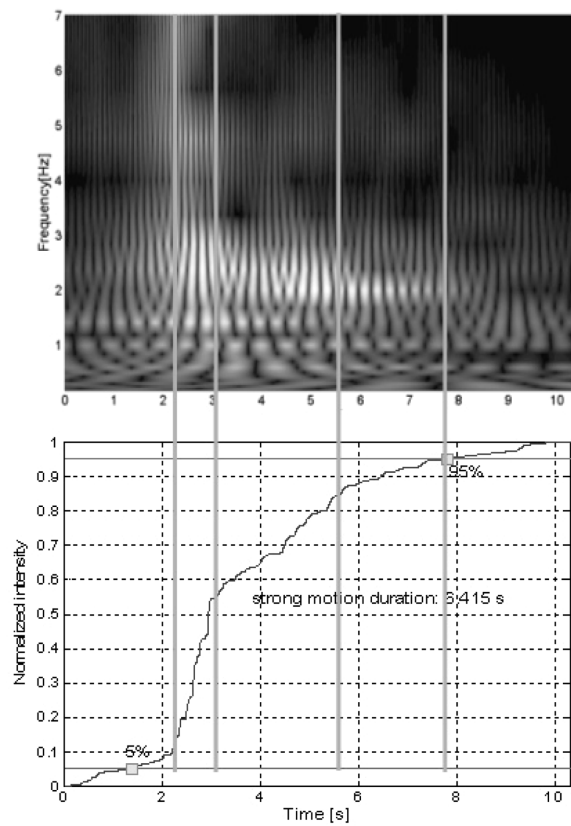


Fig. 18 Wavelet map and Husid plot of the modified record of the Coalinga earthquake

energy between 2.2 and 3 seconds, followed by a smaller slope (i.e., smaller rate of energy increase) between 3 and 5.7 seconds. The slope decreases further after 5.7 until 7.8 seconds. Observing the

frequency decomposition in the wavelet map in Fig. 18 one can see that there is a dominant frequency of about 2-3 Hz in the first zone (2.2 to 3 seconds), it decreases from 3 to 5.7 seconds, and then slightly diminishes from 5.7 to 7.8 seconds.

In order to be compatible to a design spectrum, the modified accelerogram usually needs to have a frequency content richer than that of the original signal. This is so because the usual design spectra have a high plateau extending from short to medium periods and it is unlikely that a real earthquake record will have component waves of similar intensities in this range of periods. The matching procedure thus needs to amplify the components in this range. As it was explained, the proposed procedure does not create or add new components to the original signal: it just amplifies (or reduces, depending on the case) those component waves already present. Therefore, when it increases the weight of some components, the strong motion phase of the original accelerogram will practically always be stretched. A means to partially inhibit the increase in the strong motion duration is presented in the last section of the paper.

8. Energy content of the modified records

For energy-based seismic design, it is important to estimate the input energy to the structure and distribute it to its various structural components. Housner (1956) was probably the first researcher to recommend an energy approach for earthquake resistant design. He pointed out that when the ground motion transmits energy into the structure, some of this energy is dissipated through damping and nonlinear behavior, and the remaining is stored in the structure in the form of kinetic and elastic strain energy. Housner computed the input energy E_i per unit mass as

$$\frac{E_i}{m} = \frac{1}{2}(PSV)^2 \quad (37)$$

where m is the oscillator mass and PSV denotes the pseudo-spectral velocity. Eq. (37) can be used to define the input energy spectrum associated with a given accelerogram. This spectrum provides another means to characterize the spectrum-compatible earthquake records.

Fig. 19(a) shows the input energy spectra for the original and the modified record of the Coalinga earthquake. The spectrum of the modified record exhibits a high level of input energy spread over a very wide range of periods. On the contrary, the input energy spectrum of the original record drops rapidly for high periods. This mismatch between the energy spectra of real and artificial records was the focus of criticism for using artificial accelerogram (Naeim and Lew 1995). The shape of the input energy spectrum of the compatible accelerogram obtained by modifying the Friuli record is typical of all the artificial records. This is expected since the pseudo-spectral velocity is related to the pseudo-spectral acceleration (PSA)

$$PSV(T) = \left(\frac{T}{2\pi}\right)PSA(T) \quad (38)$$

and thus it is obvious that any record compatible with a target design spectrum $PSA(T)$ will have an input energy spectrum that is approximately given by

$$\frac{E_i}{m} = \frac{1}{8\pi^2}(T*PSA)^2 \quad (39)$$

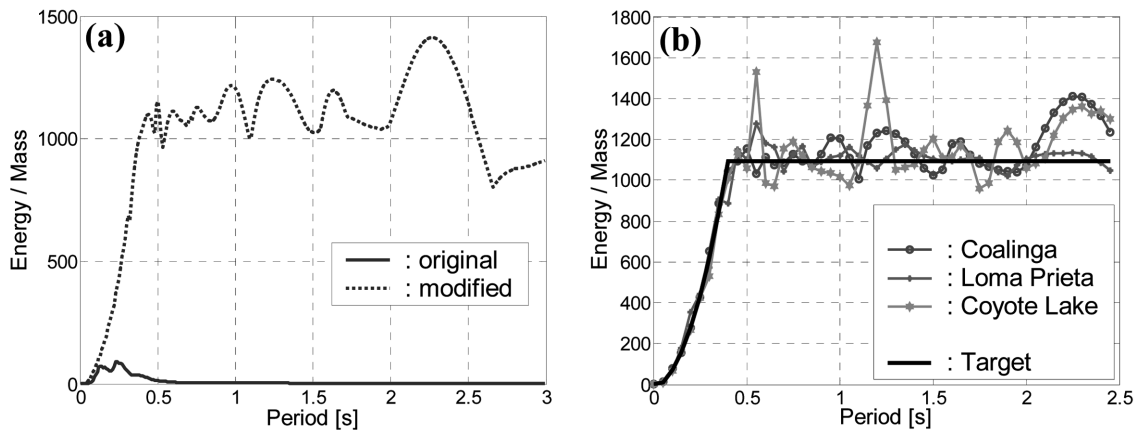


Fig. 19 The input energy spectra of the original and modified record of the Coalinga earthquake (a), and the energy spectra of the UBC-95 design spectrum and three modified records (b)

This behavior can be seen in Fig. 19(b) which shows the input energy spectra of the three modified records and the corresponding spectrum obtained with Eq. (39). The latter can be regarded as the input energy spectrum associated with a code design spectrum, in this case the one prescribed by the UBC-97. Indeed there is a discrepancy between the input energy spectra of real records and those of artificial accelerograms. However, this is caused by the shape of the pseudo acceleration design spectrum. If one accepts the design spectrum as the fundamental tool for earthquake resistant design, then one has to abide by the discrepancy. The spectrum-matching procedure is not responsible for the incongruity in the input energy spectra of real and artificial records: it is implicit in the currently used design spectra.

9. The two-band matching procedure

It was demonstrated that by using the matching procedure the temporal variations of the frequency content of the original record were not completely retained in the compatible record. Therefore, an alternative way to match a target spectrum is investigated next.

The spectrum matching scheme used for the new application is the same iterative procedure proposed before. However, this time the original record will be modified to match only a specific part of the target spectrum, based on the characteristics of the record. As a consequence, to match the design spectrum along the full period range it is necessary to modify more than one record, each one matching different parts of the target spectrum. For practical reasons, however, the span of spectrum periods will be divided in only two bands.

To demonstrate the numerical implementation of the two-band matching procedure, the records of two earthquakes with epicenters close and faraway from the site were selected. The first record corresponds to the Friuli earthquake (Italy 1976) measured at Forgario Cornino station with a closest distance to the rupture failure of 13 km and a USGS Site Classification B. The second accelerogram belongs to the Loma Prieta earthquake (California 1989) registered at Treasure Island station with a closest distance to the rupture failure of 82.9 km and a USGS Site Classification D. Fig. 20 displays the response spectra of the original accelerograms together with the design

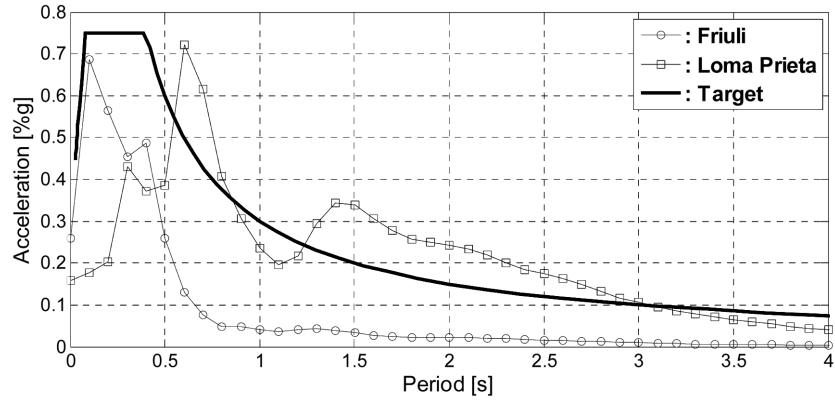


Fig. 20 Response spectra of the Treasure Island record of the Loma Prieta earthquake and the Forgario Cornino record of the Friuli earthquake together with the UBC-97 spectrum

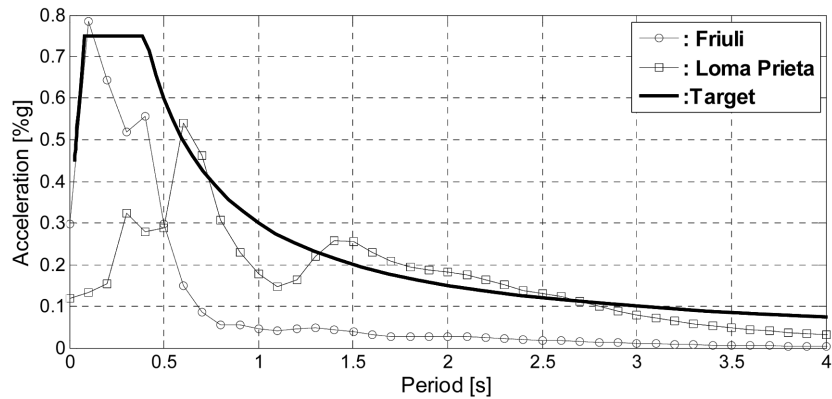


Fig. 21 Response spectra for the scaled records of the Loma Prieta earthquake at Treasure Island station and the Friuli earthquake at Forgario Cornino station with the UBC-97 spectrum

spectrum of the UBC-97 for seismic zone 3 and soil type S_B , which will be used as target. Of course, in a real application, the selection of the two records must be done with caution. In order for the procedure to provide meaningful results, each accelerogram must be representative of a near fault and distant fault seismic events.

Once the two earthquakes records are selected, the next step is to scale their response spectra by an appropriate factor to allow one to visualize the period ranges where each record must be modified to match the target spectrum. Fig. 21 shows the scaled response spectra of the Friuli record modified by a factor of 1.1 and the Loma Prieta record scaled by 0.70. Based on the results of Fig. 21, the record of Friuli will be modified to match the target spectrum in the range 0 to 0.45s whereas the record of Loma Prieta will be modified for the same purpose in the period range 0.55 to 4s. The response spectra of the two accelerograms after they are modified with the wavelet based procedure are shown in Fig. 22.

Fig. 23 (a and b) shows the accelerograms of the Friuli earthquake before and after the matching procedure was applied. At a first glance, both accelerograms appear to have similar general shapes; for instance both have their maximum peak acceleration at the same time, 3.8 seconds. The Husid

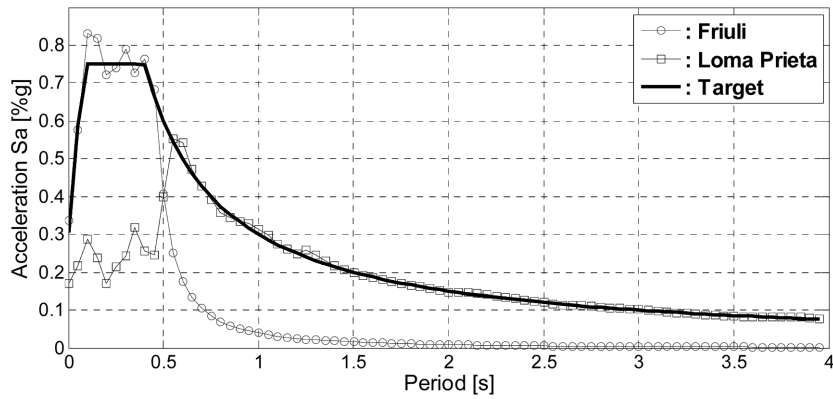


Fig. 22 Response spectra for the modified records of the Loma Prieta earthquake at Treasure Island Station and the Friuli earthquake at Forgario Cornino station with the UBC design spectrum

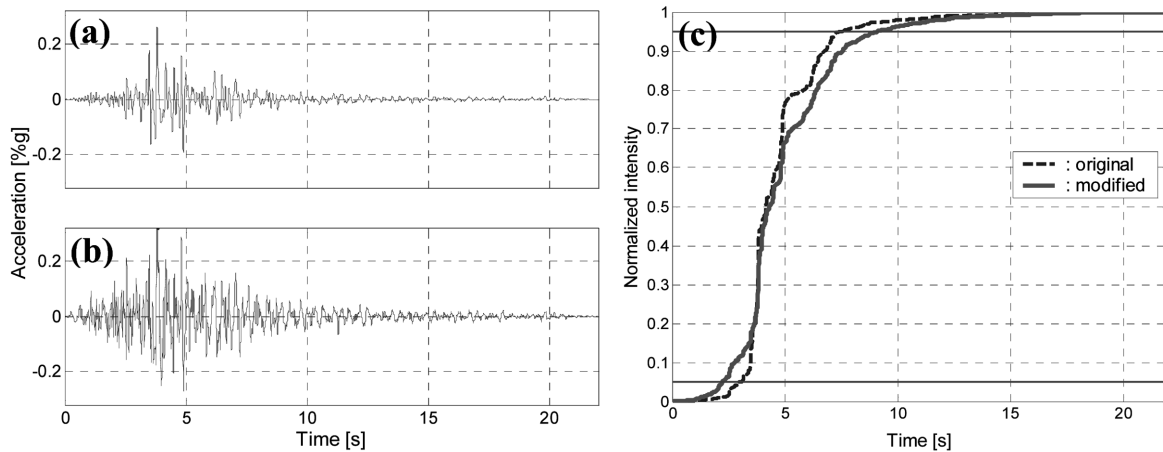


Fig. 23 Original (a) and modified (b) accelerogram of the Friuli earthquake with its Husid plots (c)

plots can help to make a more specific, qualitative comparison. Fig. 23(c) displays these plots for the original and modified accelerograms of the Friuli earthquake. The strong motion duration (calculated as explained before) after the modification was increased by approximately two seconds (from 4.5 to 6.8 seconds). Moreover, the general trend of the Husid plots of the two records is quite similar.

Additional information is provided by the Fourier spectra of the original and modified accelerograms depicted in Fig. 24. Although the two spectra look different, some important characteristics of the original record still remain in the modified accelerogram. For instance, the dominant frequency for both accelerograms is between 2-3 Hz and almost all the frequency content of the accelerograms is between 2-10 Hz.

Fig. 25 presents the wavelet map of the two accelerograms of the Friuli earthquake. It can be observed from this figure that the non-stationary characteristics of the original accelerogram are still present in the modified accelerogram.

The next set of figures present similar results but for the Loma Prieta record. Fig. 26 (a and b)

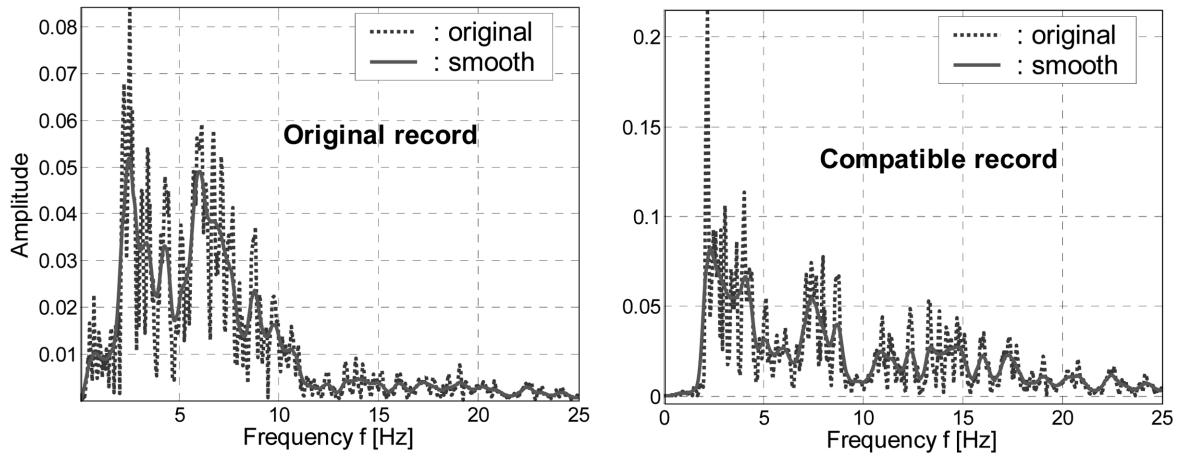


Fig. 24 Fourier spectrum of the original and modified record of the Friuli earthquake

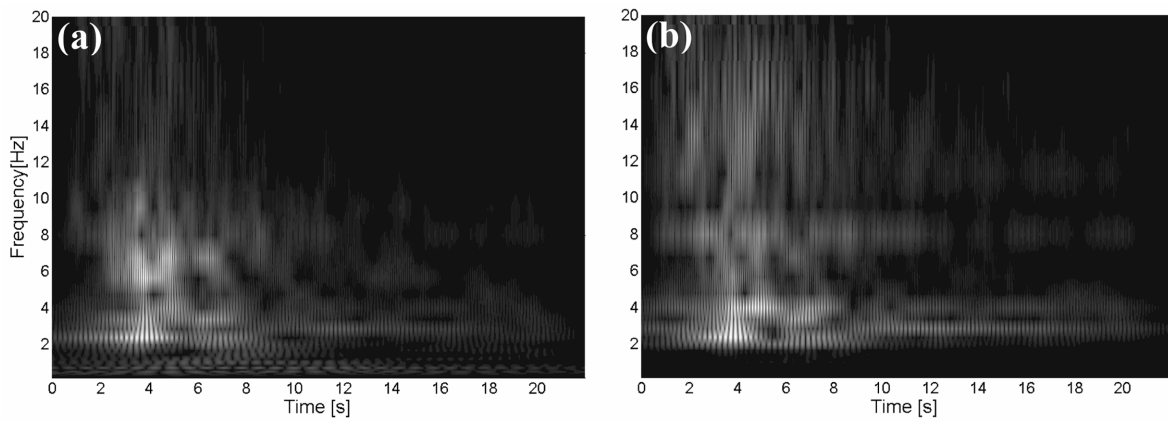


Fig. 25 Wavelet map of the original (a) and modified (b) record of the Friuli earthquake

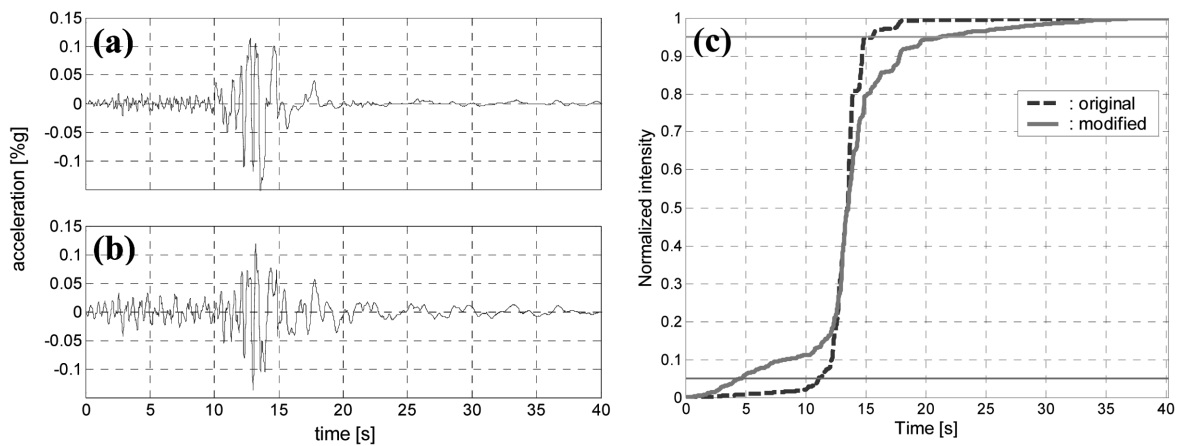


Fig. 26 Original (a) and modified (b) accelerogram of the Loma Prieta earthquake with its Husid plots (c)

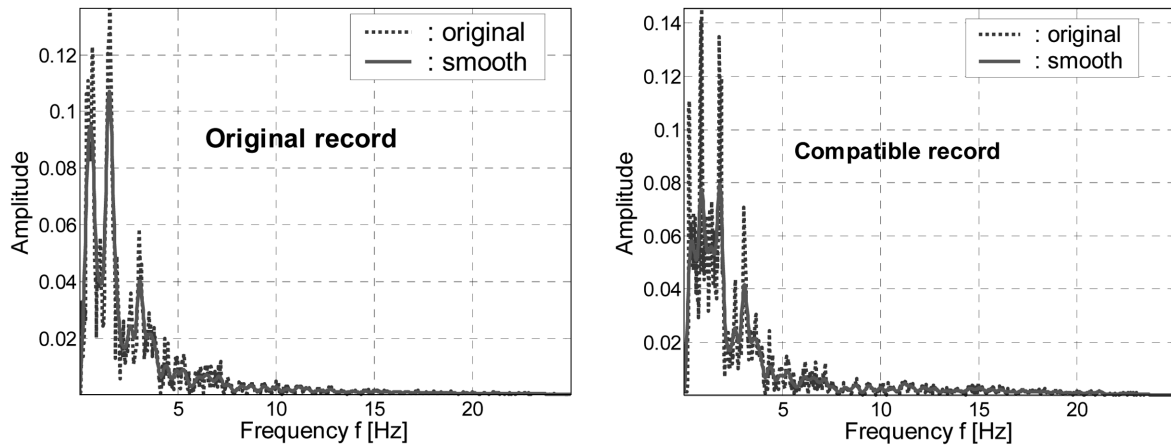


Fig. 27 Fourier spectrum of the original and modified record of the Loma Prieta earthquake

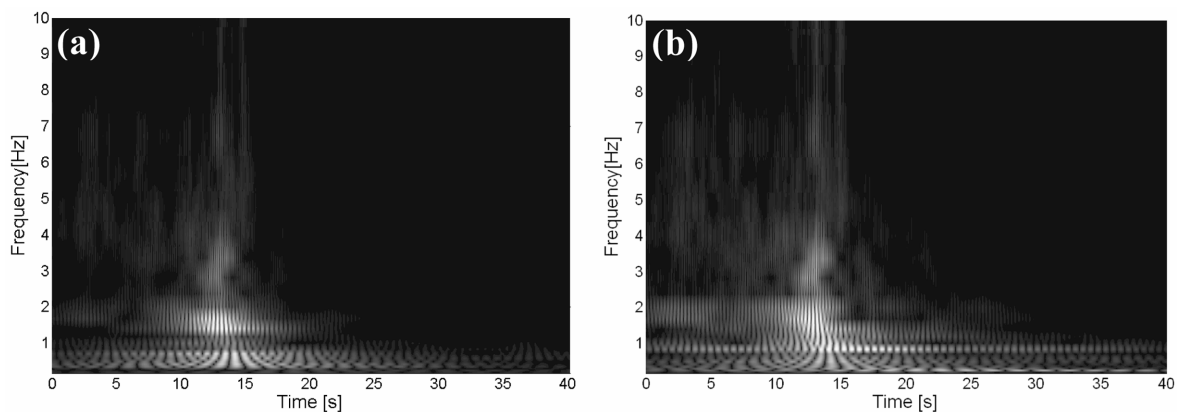


Fig. 28 Wavelet map of original (a) and modified (b) record of the Loma Prieta earthquake

shows the accelerogram of the Loma Prieta earthquake before and after it was modified to match the long period zone of the target spectrum. As it happened with the Friuli earthquake, it can be verified from this figure that both accelerograms have a similar general shape. The two accelerograms have maximum amplitudes between 12 and 14 seconds. Fig. 26(c) displays the Husid plot of the original and modified accelerograms of the Loma Prieta earthquake. Even though the strong motion duration in the modified record was increased by almost twelve seconds (from 4.5 to 15.6 seconds), the shape of the Husid plot of both records between 12 and 15 seconds is very similar.

The Fourier spectra of the original and modified accelerogram of the Loma Prieta earthquake are shown in Fig. 27. Both spectra look very similar: practically all the frequency content of the accelerograms is between 0.2 to 5 Hz and the dominant frequencies are in the range from 0.2 to 2 Hz. Fig. 28 shows the wavelet map of the Loma Prieta accelerograms. Although the task of comparing these two-dimensional plots is not as straightforward as with the Fourier spectra, it can be seen that both wavelet maps are quite similar. Therefore, the two-band matching procedure helped to reduce to some extent the alteration of the characteristics of the original records, albeit not completely.

10. Conclusions

The continuous wavelet transform was applied in an iterative scheme to modify historic earthquake records so that they become compatible with a prescribed design spectrum. The procedure converges quickly and accurately to the desired target spectrum. The wavelet transform was also used for the time-frequency analysis of the modified earthquake records. This tool can provide information about how the frequency content of the spectrum-compatible accelerograms evolves with time and, in general, shed light on how the original records were altered. The same ideas can be applied for the analysis of real records.

After processing the records with the wavelet procedure, they no longer have zero end displacement and velocity. Hence, a baseline correction scheme originally proposed by Wilson (2001) was described and applied to rectify the compatible accelerograms. This method does not modify the frequency content and the corrected accelerograms are still compatible with the target spectrum.

An alternative way to match a design spectrum, referred to as the “two band matching procedure” was presented. It is based on using two earthquake records with different characteristics to match the short period and long period zones of the design spectrum. It was verified that the new spectrum compatible records are able to better preserve the original attributes of the historical records.

Acknowledgements

The work described in this paper was supported by the Puerto Rico Strong Motion Program under the direction of Dr. José Martínez-Cruzado. This support is gratefully acknowledged.

References

- Arias, A. (1970), “A measure of earthquakes intensity”, *Seismic Design for Nuclear Power Plants*, Hansen, R., Ed., MIT Press, Cambridge, Massachusetts, 438-483.
- Bommer, J.J. and Ruggieri, C. (2002), “The specification of acceleration time-histories in seismic codes”, *Eur. Earthq. Eng.*, **16**(1), 3-16.
- Bommer, J.J. and Scott, S.G. (2000), “The feasibility of using real accelerograms for seismic design”, *In Implications of Recent Earthquakes on Seismic Risk*, Elnashai and Antoniou, Eds., Imperial College Press, UK, 115-126.
- Converse, A.M., Brady, A.G. and Joyner, W.B. (1984), “Improvements in strong-motion data processing procedures”, *Proc. of the 8th World Conf. on Earthquake Engineering*, San Francisco, California, 143-148.
- Hancock, J., Watson-Lamprey, J., Abrahamson, N.A., Bommer, J.J., Markatis, A., McCoy, E. and Mendis, R. (2006), “An improved method of matching response spectra of recorded earthquake ground motion using wavelets”, *J. Earthq. Eng.*, **10**, special issue 1, 67-89.
- Housner, G.W. (1956), “Limit design of structures to resist earthquakes”, *Proc. of the 1st World Conf. on Earthquake Engineering*, Los Angeles, California, 1956, 5.1-5.13.
- International Conference of Building Officials. *Uniform Building Code* – 1997 Edition, ICBO, Whittier, California.
- Lilhanand, K. and Tseng, W.S. (1988), “Development and application of realistic earthquake time histories compatible with multiple-damping design spectra”, *Proc. of the 9th World Conf. of Earthquake Engineering*, Tokyo-Kyoto, Japan.

- Mahin, S.A. (1984), "Effects of duration and aftershocks on inelastic design earthquakes", *Proc. of the 8th World Conf. in Earthquake Engineering, San Francisco, California*, 881-888.
- Malhotra, P.K. (2003), "Strong motions records for site-specific analysis", *Earthq. Spectra*, **19**(3), 557-578.
- Misiti, M., Misiti, Y., Oppenheim, G. and Poggi, J.-M. (2000), *Wavelet Toolbox User's Guide*, The Math Works Inc., Natick, Massachusetts.
- Montejo, L. (2004), *Generation and Analysis of Spectrum-Compatible Earthquake Time-Histories using Wavelets*, MS Thesis, University of Puerto Rico at Mayagüez, Mayagüez, Puerto Rico.
- Mukherjee, S. and Gupta, V.K. (2002), "Wavelet – Based characterization of design ground motions", *Earthq. Eng. Struct. Dyn.*, **31**(5), 1173-1190.
- Naeim, F. and Lew, M. (1995), "On the use of design spectrum compatible time histories", *Earthq. Spectra*, **11**(1), 111-127.
- Peng, Z., Chu, F. and He, Y. (2002), "Vibration signal analysis and feature extraction based on reassigned wavelet scalogram", *J. Sound Vib.*, **253**(5), 1087-1100.
- Rizzo, P.C., Shaw, D.E. and Jarecki, S.J. (1975), "Development of real/synthetic time histories to match smooth design spectra", *Nucl. Eng. Des.*, **32**, 148-155.
- Suarez, L.E. and Montejo, L.A. (2003), "Generación de registros artificiales compatibles con un espectro de respuesta mediante la transformada wavelet", *Proc. of the II Congreso Nacional de Ingeniería Sísmica*, Medellín, Colombia.
- Suárez, L.E. and Montejo, L.A. (2005), "Generation of artificial earthquakes via the wavelet transform", *Int. J. Solids Struct.*, **42**(21-22), 5905-5919.
- Trifunac, M.D. and Brady, A.G. (1975), "A study on the duration of strong earthquake ground motion", *B. Seismic Soc. Am.*, **65**, 581-626.
- Trifunac, M.D. and Lee, V.W. (1979), *Routing Processing of Strong-Motion Accelerograms*, California Institute of Technology, Earthquake Engineering Research Laboratory, Report No. EERL 73-03, Pasadena, California.
- Tse, P.W., Yang, W. and Tam, H.Y. (2004), "Machine fault diagnosis through an effective exact wavelet analysis", *J. Sound Vib.*, **277**, 1005-1024.
- Vanmarcke, E.H. and Gasparini, D.A. (1976), *Simulated Earthquake Motions Compatible with Prescribed Response Spectra*, Report 76-4, Dept. of Civil Engineering, Massachusetts Institute of Technology, Cambridge, Massachusetts.
- Wilson, W.L. (2001), *Three-Dimensional Static and Dynamic Analysis of Structures: A Physical Approach with Emphasis on Earthquake Engineering*, Third Edition, Computers and Structures Inc., Berkeley, California, 2001.